

Accuracy of bead-spring chains in strong flows

Patrick T. Underhill, Patrick S. Doyle*

Department of Chemical Engineering, Massachusetts Institute of Technology, Cambridge, MA, United States

Received 23 August 2006; received in revised form 9 April 2007; accepted 21 May 2007

Abstract

We have analyzed the response of bead-spring chain models in strong elongational flow as the amount of polymer represented by a spring is changed. We examined the longest relaxation time of the chains which is used to quantify the strength of the flow in terms of a Weissenberg number. A chain with linear springs can be used to predict the longest relaxation time of the nonlinear chains if the linear spring constant is modified correctly. We used the expansion of the elongational viscosity in the limit of infinite Weissenberg number to investigate the change of the viscosity as the scale of discretization was changed. We showed that the viscosity is less sensitive to the details of the spring force law because the chain is fully extended at very large Weissenberg number. However, the approach to that infinite Weissenberg number response is dependent both on the behavior of the spring force at large force and the behavior at small force. New spring force laws to represent the worm-like chain or the freely jointed chain are correct at both of these limits, while other currently used force laws produce an error. We also investigated the applicability of these expansions to chains including hydrodynamic interactions. Our results suggest that the longest relaxation time may not be the appropriate time scale needed to non-dimensionalize the strain rate in such highly extended states.

© 2007 Elsevier B.V. All rights reserved.

Keywords: Coarse-graining; Bead-spring models; Elongational flow

1. Introduction

Bead-spring chain models have become common coarse-grained versions of polymers. Most recent studies aimed at increasing the accuracy of bead-spring chains have concentrated on the inclusion of excluded volume and hydrodynamic interactions [1–3]. These can now be included in the simulations because of increases in computation power and methods of algorithm speed-up. While work in this area has furthered our understanding of and confirmed the importance of excluded volume and hydrodynamic interactions, we consider here the role of the spring force law. The increase in computation power has also allowed for the use of a large number of springs where each spring represents a small segment of polymer. The use of “small” springs has been motivated in part by many new microfluidic applications in which the behavior at a small length scale is critical [4–6]. Coarse-graining out these finer-scale details gives inaccurate models. It has been shown that using the conventional spring force laws at this high discretization can result in significant errors [7–9]. Thus, understanding the validity

of currently used force laws and how to correct them when needed is an important aspect of building an accurate polymer model.

New spring force laws have been developed which do not have these errors at high discretization [7–9]. By construction these new bead-spring chains have the same force-extension behavior as the micromechanical models they represent. The response in low Weissenberg number flow due to the force law has also been studied in detail. By relating the contribution of the force law to the force-extension behavior at small force, we could illustrate the advantages of the new force laws. While the advantages of the new force laws for the force-extension behavior at large force is clear, the impact in strong flows has not been explicitly examined. One difference between the force-extension behavior at large force and strong flows is the parameter used to quantify the external forcing. In force-extension behavior, the appropriate scale for the external force is $k_B T / A_p$, where A_p is the persistence length. However, the strength of the flow is typically specified in terms of a Weissenberg number, $Wi = \dot{\epsilon} \tau$, where $\dot{\epsilon}$ is the strain rate and τ is the polymer's longest relaxation time. This makes the analysis in flow more complicated to understand because the longest relaxation time itself depends on the discretization error of the spring force laws [10]. However, even if the longest relaxation time of the bead-spring chain dif-

* Corresponding author.

E-mail address: pdoyle@mit.edu (P.S. Doyle).

fers from the polymer to be modeled, one would think that if the strain rate is correspondingly changed to simulate at the same Wi , the difference will not play a role. For this reason we will take care to calculate the longest relaxation time of the bead-spring chains and examine how the response changes with the Wi held fixed.

Here we will examine the response of bead-spring chains in strong steady uniaxial extensional flow, comparing the behavior of previous force laws with those which have been recently developed. There has been much work recently looking at the response of bead-spring chain models in extensional flow. Simulations in uniaxial and planar extensional flow can be compared directly with experiments done with a filament stretching device or cross-slot devices [11,12]. Here we will be focusing on the effect of the spring force law on the response when the polymer is strongly stretched (approaching full extension). In such states the inclusion of excluded volume effects should not affect the response because the likelihood that the chain will be in a configuration which is influenced by the excluded volume is small due to the strong stretching. Recently, Sunthar et al. [13] examined the response in the start-up of elongational flow including excluded volume interactions. While they found that excluded volume interactions are important at small strains, we consider here only the steady response (or infinite strain value). This steady value will not be affected by excluded volume interactions similar to force-extension behavior [14].

Initially, we will also neglect the influence of hydrodynamic interactions. In an extended configuration, the segments of polymer are further apart so the hydrodynamic interactions will be weaker than in the equilibrium coiled state. However, when expressing the flow strength in terms of a Weissenberg number, the longest relaxation time is used. This longest relaxation time is affected by hydrodynamic interactions and even excluded volume interactions. We will briefly examine the impact of hydrodynamic interactions and their impact on the response in strong extensional flow.

2. Bead-spring models

In this study we have examined a number of different spring force laws. Two of the most common nonlinear spring force laws are the FENE and Marko–Siggia force laws. The FENE force law is an approximation to the inverse Langevin function. Researchers have also used a Padé approximation to the inverse Langevin. We will compare the response of these force laws with two new force laws that we have developed to model the freely jointed chain and worm-like chain [8,9]. We have used the same notation and non-dimensionalization as in ref. [7], which we briefly review here.

The Marko–Siggia force law is an approximation to the response of long worm-like chains. The spring force is

$$f_s(r) = \left(\frac{k_B T}{A_{\text{eff}}} \right) \left\{ \hat{r} - \frac{1}{4} + \frac{1}{4(1 - \hat{r}^2)} \right\} \quad (1)$$

where ℓ is the fully extended length of a spring, $\hat{r} = r/\ell$ the fractional extension of the spring, and A_{eff} is the effective per-

sistence length. The true persistence length of the polymer being modeled is denoted A_{true} . The key dimensionless parameters are $\nu \equiv \ell/A_{\text{true}}$ which is the number of persistence lengths represented by each spring and $\lambda \equiv A_{\text{eff}}/A_{\text{true}}$ which is a correction factor that can be used to correct the polymer response. The use of this correction factor is discussed in ref. [7]. Different criteria exist for choosing λ as a function of ν . In particular we will be discussing the so-called low-force and high-force criteria. These are choices for λ as a function of ν such that the force-extension behavior of the bead-spring chain matches the micromechanical model at low or high force, respectively.

In ref. [9] we have developed a new force law which models the worm-like chain

$$f_s(r) = \left(\frac{k_B T}{A_{\text{eff}}} \right) \left\{ \frac{\hat{r}}{(1 - \hat{r}^2)^2} - \frac{7\hat{r}}{\nu(1 - \hat{r}^2)} + \left(\frac{3}{32} - \frac{3}{4\nu} - \frac{6}{\nu^2} \right) \hat{r} + \left(\frac{(13/32) + (0.8172/\nu) - (14.79/\nu^2)}{1 - (4.225/\nu) + (4.87/\nu^2)} \right) \hat{r}(1 - \hat{r}^2) \right\}. \quad (2)$$

This force law reproduces the force-extension behavior of the worm-like chain by construction both at low and high forces.

We have also examined spring force laws which represent freely jointed chains. The FENE force law is an approximation to the response of long freely jointed chains [15]. The spring force is

$$f_s(r) = \left(\frac{3k_B T}{a_{K,\text{eff}}} \right) \frac{\hat{r}}{1 - \hat{r}^2}, \quad (3)$$

where $a_{K,\text{eff}}$ is the effective Kuhn length of the polymer. To non-dimensionalize the equations we define an effective length over which the chain is rigid, A_{eff} . Although this length needs to be proportional to the Kuhn length, the proportionality constant can be chosen arbitrarily to make the equations look simpler. Obviously the response of the chain will be independent of this choice, though the dimensionless equations will depend on the choice made. For convenience with the FENE force law we take it to be $A_{\text{eff}} = a_{K,\text{eff}}/3$. We similarly have that $A_{\text{true}} = a_{K,\text{true}}/3$ where $a_{K,\text{true}}$ is the true Kuhn length of the polymer. With this choice, ν represents three times the number of Kuhn lengths represented by each spring. One advantage of this choice is that it removes any overall prefactor in the dimensionless spring force formula. It also means that there is a correspondence $b \leftrightarrow \nu/\lambda$, where b is a common parameter used in the literature which uses the FENE force law.

An alternative to the FENE force law which is seeing increasing use is a Padé approximation to the inverse Langevin function due to Cohen [16], which is

$$f_s(r) = \left(\frac{3k_B T}{a_{K,\text{eff}}} \right) \frac{\hat{r} - \hat{r}^3/3}{1 - \hat{r}^2}. \quad (4)$$

The advantage of this force law is that it more accurately approximates the inverse Langevin function. In particular, the force has the same divergence as the inverse Langevin function. Although the FENE force is correctly proportional to $(1 - r/\ell)^{-1}$ near full extension, the proportionality factor is incorrect. The Cohen

form has the same proportionality factor as the inverse Langevin function. We will return to this difference between the FENE and Cohen force laws when analyzing the steady, strong flows.

We have also previously developed a new spring force law which is a better approximation to the response of the freely jointed chain [8] which is given by

$$f_s(r) = \left(\frac{k_B T}{a_K} \right) \frac{(3 - 10/\nu + 10/(3\nu^2))\hat{r} - (1 + 2/\nu + 10/(3\nu^2))\hat{r}^3}{1 - \hat{r}^2} \quad (5)$$

3. Brownian dynamics

We use the method of Brownian dynamics (BD) to calculate the response of bead-spring chains in non-equilibrium situations. This technique has been used widely to calculate the response of bead-spring chains [17,11]. The technique integrates forward in time the equation of motion, a stochastic differential equation. This equation is given by

$$m_i \ddot{\mathbf{r}}_i = \mathbf{F}_i^{\text{net}} = \mathbf{F}_i^{\text{B}} + \mathbf{F}_i^{\text{d}} + \mathbf{F}_i^{\text{s}} \approx \mathbf{0}, \quad (6)$$

where the subscript i denotes bead i , m the mass of each bead, $\ddot{\mathbf{r}}$ the acceleration, \mathbf{F}^{net} the net force, \mathbf{F}^{B} the Brownian force due to collisions of the solvent molecules with the beads, \mathbf{F}^{d} the drag force due to the movement of each bead through the viscous solvent, and \mathbf{F}^{s} is the systematic force on each bead due to the springs and any external forces. We neglect the inertia (mass) of the beads, and so the net force is approximately zero.

For simulations near equilibrium and if each spring represented a large segment of polymer, it was sufficient to use a simple Euler integration scheme. However, at large Weissenberg number and if each spring represented a small segment of polymer, the timestep would need to be so small that the simulations became too computationally expensive. In these situations we used the semi-implicit predictor-corrector method developed by Somasi et al. [10]. For the simulations including hydrodynamic interactions, we used the Rotne–Prager–Yamakawa tensor [18,19] and the generalization of the integration method due to Hsieh et al. [2]. We found that using a look-up table with linear interpolation in the semi-implicit method introduced an error when used at large Weissenberg number. Therefore, a look-up table was not used.

4. Longest relaxation time

When examining the behavior of bead-spring chains in flow, it is common to express the flow conditions (shear rate or elongation rate) in terms of a Weissenberg number. The Weissenberg number (Wi) is taken as the product of the shear rate or elongation rate and the longest relaxation time. This longest relaxation time will certainly be affected by excluded volume and hydrodynamic interactions. However, for consistency with the high Wi calculations to be done without those effects, we consider the longest relaxation time of models without EV or HI. For models for which analytic calculations can be performed such as for lin-

ear springs, the longest relaxation time can be expressed exactly as a function of the model parameters (such as the bead drag coefficient and spring constant). For nonlinear spring models, such an analytic formula for the longest relaxation time is not possible.

The longest relaxation time for these models can be calculated numerically using dynamical simulations such as BD. These simulations can be computationally costly, particularly for long chains that have long relaxation times. It is also inconvenient to have to perform a preliminary simulation for each set of model parameters before performing the primary simulations. One way around this is to use instead the characteristic time from dividing the zero-shear rate first normal stress coefficient by two times the zero-shear rate polymer viscosity [20]

$$\tau_0 \equiv \frac{\Psi_{1,0}}{2\eta_{p,0}}. \quad (7)$$

Both of these zero-shear rate properties, provided HI is ignored, can be calculated from the retarded motion expansion coefficients [7]. For the FENE force law, these can be calculated analytically. For other force laws, such as the Marko–Siggia force law, they require numerical integration but are much less computationally costly than full BD simulations. The disadvantage of using this characteristic time is that it differs from the longest relaxation time even for chains with the relatively simple linear spring force law [21]. It is unclear how the two characteristic times are related for more complicated force laws.

It is well known that because the chains do not contain EV or HI, each measure of the characteristic time will eventually scale as N^2 as the number of beads becomes asymptotically large. However, we require more detailed knowledge than this. In this article we will be analyzing the behavior from as few as two beads to a large number of beads. We will not always be in this asymptotic limit. In particular, the point at which the chain reaches this limiting behavior will depend on the choice for characteristic time.

Another way of estimating the longest relaxation time is to use the linear force law formula [11]. The linear spring constant is taken from the nonlinear spring law at small extensions, where the spring law looks linear. If the chain, as it is relaxing back to equilibrium, only samples the linear region of the spring at long times, then this should be a good approximation. It has been shown that this approximation can result in significant errors. This error results because even at equilibrium, the springs can sample the nonlinear parts of the force law as discussed in ref. [7].

Because of the deficiencies of each approximate method, we performed direct BD simulations of the relaxation of chains over a wide parameter range and with both the FENE and Marko–Siggia force laws. In order to calculate the longest relaxation time, the chains were started in a stretched configuration (95% extension) in the z direction. The chains were simulated as they relaxed back to equilibrium. At long time, the stress difference $\sigma_{zz} - \sigma_{xx}$ decays as a single exponential, $\exp(-t/\tau)$. A least-squares fit is used to extract the value of the longest relaxation time. Before plotting the results of the simulations, we will review what we call the Rouse relaxation time of a chain

and express it in the notation used here. Consider a chain of N beads connected by $N - 1$ linear springs with spring force law $f_s(r) = Hr$. The longest relaxation time of the chain is

$$\tau = \frac{1}{2 \sin^2(\pi/(2N))} \frac{\zeta}{4H}. \quad (8)$$

Now, consider a chain of inextensible springs. Using the notation from ref. [7], we write the Taylor expansion of the spring force as

$$f_s(r) = \frac{k_B T 2 \phi_2 \nu}{\ell^2 \lambda} r + \mathcal{O}(r^2) \quad (9)$$

If we treat the linear term like the linear spring, the longest relaxation is what we call the Rouse time

$$\tau_R = \frac{1}{2 \sin^2(\pi/(2N))} \frac{\zeta \ell^2 \lambda}{8 \phi_2 k_B T \nu}. \quad (10)$$

With our choice of A_{true} as the persistence length then $\phi_2 = 3/4$ for the Marko–Siggia force law, and with A_{true} as one-third of the Kuhn length then $\phi_2 = 1/2$ for the FENE force law. Note that because of our ability to take different choices for A_{true} the formulas can appear to take different forms. However, because any change of choice affects the meaning of ν while also changing the value of ϕ_2 , the physical meaning of a formula remains invariant. To illustrate this, let us insert into the Rouse time the definitions of ν and λ and the value of ϕ_2 . For the Marko–Siggia force law, we have taken A_{eff} to be the effective persistence length, $A_{p,\text{eff}}$, and the Rouse time becomes

$$\tau_R = \frac{1}{2 \sin^2(\pi/(2N))} \frac{\zeta \ell A_{p,\text{eff}}}{6 k_B T}. \quad (11)$$

For the FENE force law, we have taken A_{eff} to be one-third of the effective Kuhn length, $a_{K,\text{eff}}/3$, and the Rouse time becomes

$$\tau_R = \frac{1}{2 \sin^2(\pi/(2N))} \frac{\zeta \ell a_{K,\text{eff}}}{12 k_B T}. \quad (12)$$

These two formulas remain the same independent of any choice for A_{true} and the corresponding value of ϕ_2 .

We now show the results of the BD simulations using the Marko–Siggia force law in Fig. 1 where the longest relaxation time of the chain is divided by the above Rouse time. The first thing to note is that the longest relaxation time is the same as the Rouse time when $\nu/\lambda \rightarrow \infty$ but deviates for smaller values. This is because the Rouse time assumes that near equilibrium the spring only samples the low extension (linear) part of the spring. As discussed in ref. [7] if ν/λ is not infinite, the spring samples the nonlinear parts of the spring even at equilibrium. However, the other important aspect to notice from Fig. 1 is that the relaxation time scales with N just like the Rouse result. The deviation from the Rouse time is only a function of ν/λ . This suggests that it is possible to describe the relaxation time using a chain with linear springs, but which have a linear spring constant that differs from that in Eq. (9). In some approximate sense, the chain still responds linearly to external forces even if the spring samples the nonlinear regions and so returns to equilibrium using some effective linear restoring force. This is reminiscent of the force-extension behavior of the chains seen

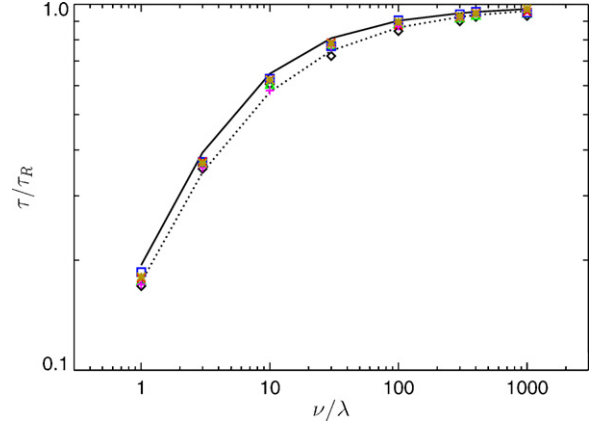


Fig. 1. Plot of the longest relaxation time of Marko–Siggia bead-spring chains relative to the Rouse prediction as a function of the number of effective persistence lengths each spring represents. The symbols represent different number of beads: $N = 2$ (diamond), $N = 5$ (triangle), $N = 10$ (square), $N = 30$ (\times), $N = 50$ ($+$), and $N = 100$ ($*$). The solid line is the modified Rouse relaxation time (Eq. (18)). The dotted line is the fitted function (Eq. (21)).

in ref. [7]. Even if the chain samples the nonlinear regions, the force-extension behavior is linear at low force. Ref. [7] showed that a bead-spring chain has

$$\lim_{f \rightarrow 0} \frac{\partial}{\partial f} \langle z_{\text{tot}} \rangle_m = \frac{(N-1)\ell^2 \langle \hat{r}^2 \rangle_{\text{eq}}}{3k_B T}, \quad (13)$$

where $\langle z_{\text{tot}} \rangle_m$ is the average z extension of the model. The spring force law comes in through the equilibrium averaged single spring moment

$$\langle \hat{r}^2 \rangle_{\text{eq}} = \frac{\int_0^1 d\hat{r} \hat{r}^4 \exp[-(\nu/\lambda)\hat{U}_{\text{eff}}(\hat{r})]}{\int_0^1 d\hat{r} \hat{r}^2 \exp[-(\nu/\lambda)\hat{U}_{\text{eff}}(\hat{r})]}. \quad (14)$$

The exponential is the Boltzmann factor, and the function \hat{U}_{eff} represents the non-dimensional spring potential energy

$$\frac{\nu}{\lambda} \hat{U}_{\text{eff}}(\hat{r}) = \frac{U_{\text{eff}}(r)}{k_B T}. \quad (15)$$

For a chain of linear springs, the force-extension relation is

$$\frac{\partial}{\partial f} \langle z_{\text{tot}} \rangle_m = \frac{N-1}{H}. \quad (16)$$

Comparing Eqs. (13) and (16), we define a modified Rouse model as a chain of linear springs where the spring constant is

$$H_{\text{MR}} \equiv \frac{3k_B T}{\ell^2 \langle \hat{r}^2 \rangle_{\text{eq}}}. \quad (17)$$

This statement is equivalent to choosing the linear spring constant such that it has the same equilibrium averaged end-to-end distance squared and number of beads as the nonlinear spring chain. Following from this is that they also have the same equilibrium radius of gyration and zero shear viscosity. While these equivalences do not guarantee that this modified Rouse model will have the same longest relaxation time as the nonlinear spring chain, we hope that they will be similar. Therefore, we will compare the modified Rouse relaxation time with the exact relaxation

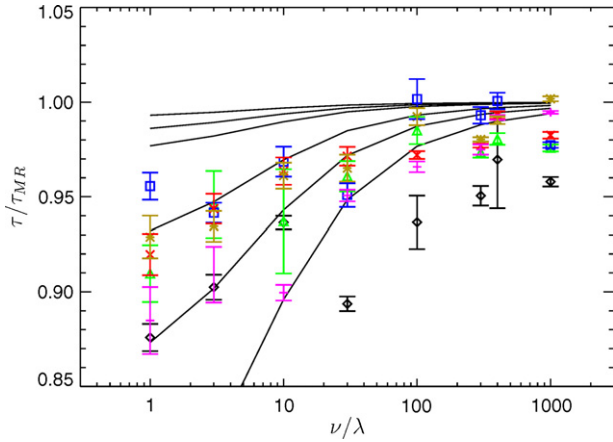


Fig. 2. Plot of the longest relaxation time of Marko–Siggia bead-spring chains relative to the modified Rouse prediction (Eq. (18)) as a function of the number of effective persistence lengths each spring represents. The symbols represent different number of beads: $N = 2$ (diamond), $N = 5$ (triangle), $N = 10$ (square), $N = 30$ (\times), $N = 50$ ($+$), and $N = 100$ ($*$). The lines represent $\tau_{0,s}$ divided by the modified Rouse prediction for the same range of number of beads, with the lowermost curve with $N = 2$ and the uppermost curve with $N = 100$. The error bars represent plus or minus two standard deviations.

time to examine how well it predicts the nonlinear chain behavior. The longest relaxation time of the modified Rouse model is

$$\tau_{MR} = \frac{1}{2 \sin^2(\pi/(2N))} \frac{\zeta \ell^2 \langle \dot{\rho}^2 \rangle_{eq}}{12k_B T}. \quad (18)$$

In Fig. 2 we show the longest relaxation times of the bead-spring chains as in Fig. 1 but now dividing the values by τ_{MR} to gauge the predictive capability of the modified Rouse model in terms of longest relaxation time. We see that the error using the modified Rouse time is much smaller than if the Rouse time were used. However, there does seem to be a general trend in which the deviation grows at smaller discretization. The modified Rouse time almost always overpredicts the values fitted from the simulations. Although the modified Rouse relaxation time does not seem to give a quantitative predictive measure, we believe it can still be used to understand the change of the longest relaxation time with a change in the scale of discretization. This is illustrated by the improved prediction of Fig. 2 compared with Fig. 1.

We should note that the Eqs. (10) and (18) are not new, and have been used before. See, for example, the review by Larson [11]. However, both equations have been called by the name ‘‘Rouse’’ because for the Rouse model, for which they were derived, they are equivalent. Our contribution is to notice that for nonlinear spring force laws, the formulas give dramatically different results. In order to carefully distinguish between these formulas which give different predictions for nonlinear springs, we call them ‘‘Rouse’’ and ‘‘modified Rouse’’, respectively. We have shown here that while the Rouse result (Eq. (10)) fails to predict the relaxation of nonlinear springs, the modified Rouse formula (Eq. (18)) retains approximate validity for nonlinear springs.

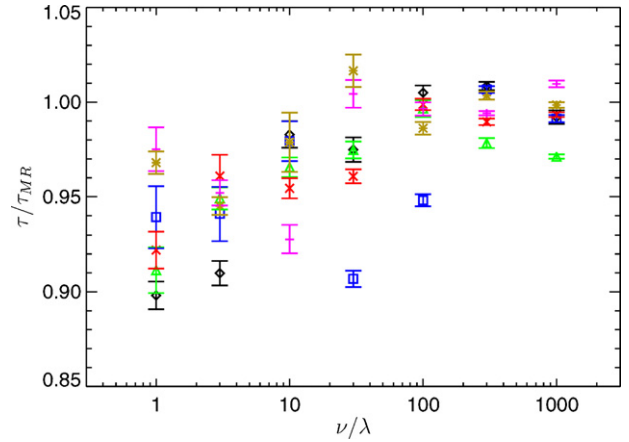


Fig. 3. Plot of the longest relaxation time of FENE bead-spring chains relative to the modified Rouse prediction as a function of the number of effective persistence lengths each spring represents. The symbols represent different number of beads: $N = 2$ (diamond), $N = 5$ (triangle), $N = 10$ (square), $N = 30$ (\times), $N = 50$ ($+$), and $N = 100$ ($*$). The error bars represent plus or minus two standard deviations.

To this point, we have compared exact BD simulations of the longest relaxation time to what we call the Rouse time (Eq. (10)) and compared the exact simulations with a modified Rouse model (Eq. (18)). The other method for estimating the relaxation time is from the ratio of zero-shear properties, Eq. (7), which we now compare with the exact BD simulations. One problem with using this estimate is that the functional dependence with N is different. For a chain of linear springs τ_0 is

$$\tau_0 = \frac{2N^2 + 7}{15} \frac{\zeta}{4H}. \quad (19)$$

This inspires us to define a scaled time

$$\tau_{0,s} \equiv \tau_0 \frac{15}{2N^2 + 7} \frac{1}{2 \sin^2(\pi/(2N))}, \quad (20)$$

which compensates for the difference in N dependence that exists even for the linear spring system. Fig. 2 also shows curves representing $\tau_{0,s}$ for the Marko–Siggia force law divided by τ_{MR} . It is not clear that $\tau_{0,s}$ represents the data any better than τ_{MR} , particularly given the accuracy of the simulations. Note also that the absolute difference between the two is quite small compared to the changes in relaxation time seen in Fig. 1. Because of the useful physical interpretation of τ_{MR} in terms of the coil size and force-extension behavior, we will not consider $\tau_{0,s}$ further. We have also performed a fit through the data to give a formula which is only slightly more accurate than τ_{MR} . For the Marko–Siggia force law, this is

$$\tau_{fit} = \frac{1}{2 \sin^2(\pi/(2N))} \frac{\zeta \ell^2}{k_B T} \frac{1}{6\nu/\lambda + 7.26\sqrt{\nu/\lambda} + 21.2}. \quad (21)$$

We have also performed BD simulations of the longest relaxation time using the FENE spring force law to verify that the trends seen with the Marko–Siggia force law are not specific to that force law. In Fig. 3 we show the longest relaxation time divided by τ_{MR} for the FENE force law. For the FENE force law the average in Eq. (18) can be calculated exactly. Therefore, the

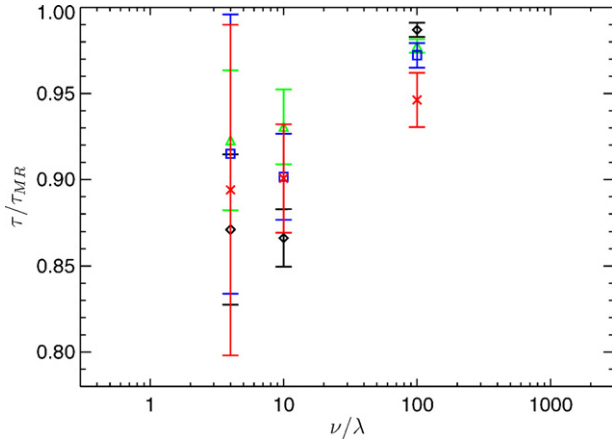


Fig. 4. Plot of the longest relaxation time of bead-spring chains using the new force law for the worm-like chain relative to the modified Rouse prediction as a function of the number of persistence lengths each spring represents. The symbols represent different number of beads: $N = 2$ (diamond), $N = 5$ (triangle), $N = 10$ (square), and $N = 30$ (\times). The error bars represent plus or minus two standard deviations.

results in Fig. 3 can be viewed as

$$\frac{\tau}{\tau_{MR}} = \frac{\tau}{\tau_R} \left(\frac{5}{\nu/\lambda} + 1 \right). \quad (22)$$

The trend is the same as with the Marko–Siggia simulations. We see a slight growing deviation at smaller discretization, however that deviation is much smaller than would be seen if the Rouse model were used to attempt to predict the simulations. The scatter of the data is of similar order of magnitude and the modified Rouse time again almost always overpredicts the simulation data. We can also perform a fit through this data to give a slightly more accurate result

$$\tau_{fit} = \frac{1}{2 \sin^2(\pi/(2N))} \frac{\zeta \ell^2}{k_B T} \frac{1}{4\nu/\lambda + 1.05\sqrt{\nu/\lambda} + 21.1}. \quad (23)$$

These fitted functions will be used later as a closed form expression for the longest relaxation time when discussing the change of the elongational viscosity with the degree of discretization.

We see that the modified Rouse formula gives a reasonable prediction of the longest relaxation time even to very high discretization. This is important because the modified Rouse formula allows us to gain intuition about the governing factors towards the relaxation time. The modified Rouse formula contains the size of a spring at equilibrium, which can be related to the force-extension response at small force. This gives us confidence that if a new spring force is used which gives the correct size of a spring and force-extension behavior, then the relaxation time will be the expected value. We can show this explicitly by calculating the relaxation time for a new force law to represent the worm-like chain (Eq. (2)). Fig. 4 shows the relaxation time of this force law divided by its modified Rouse prediction. We see the same basic result as with the Marko–Siggia and FENE force laws, that the modified Rouse formula is a reasonable prediction. A similar scatter is seen and trend to deviate more at small discretization. Note that this new force law was developed to have the correct behavior near equilibrium, and thus by construction

the modified Rouse formula is

$$\tau_{MR} = \frac{1}{2 \sin^2(\pi/(2N))} \frac{\zeta \ell A_p}{6k_B T}. \quad (24)$$

5. Steady elongational flow

After understanding the behavior of the longest relaxation time, we can investigate the high Weissenberg number response. One advantage of looking at steady elongational flow is that the viscosity can be written formally as an integral over configuration space [21]. This can be done because we are not including the effects of EV and HI, which should be of secondary importance near full extension. Although calculating the integrals numerically is not efficient for getting the exact response for chains of many springs, they can be used to develop series approximations. This same type of expansion was performed at small flow strength to obtain the retarded-motion expansion coefficients in ref. [7].

5.1. Models of the freely jointed chain

We begin our analysis of the response of bead-spring chains in strong, steady elongational flow with bead-spring chains used to model the freely jointed chain. We will be able to explicitly judge the accuracy of the coarse-grained model because the response of the freely jointed chain which is being modeled by the bead-spring chain is known.

The first bead-spring chain system we will examine to describe the behavior of the freely jointed chain is with the FENE spring force law. For the FENE force law, the expansion of the elongational viscosity in terms of Pe is

$$\tilde{\eta} \sim \tilde{\eta}_\infty - \frac{1}{Pe} \left[\left(\frac{\nu}{\lambda} + 4 \right) (N-1) - 3C_N \right] + \mathcal{O} \left(\frac{1}{Pe^2} \right), \quad (25)$$

where the Peclet number is defined as

$$Pe \equiv \frac{\dot{\epsilon} \zeta \ell^2}{k_B T}, \quad (26)$$

the dimensionless elongational viscosity is defined as

$$\tilde{\eta} = \frac{\bar{\eta} - 3\eta_s}{n_p \zeta \ell^2}, \quad (27)$$

and the dimensionless elongational viscosity at infinite Pe is

$$\tilde{\eta}_\infty = \frac{N(N^2 - 1)}{12}. \quad (28)$$

We have also defined the parameter C_N which is a function of N as

$$C_N \equiv \sum_{m=1}^{N-1} \frac{1}{1+m+m^2}. \quad (29)$$

Our approach is to use this expansion to understand the change in the response of the chain as the amount of polymer represented by a spring is changed. Using an analytic expansion will allow us to make precise statements about the effect of the different

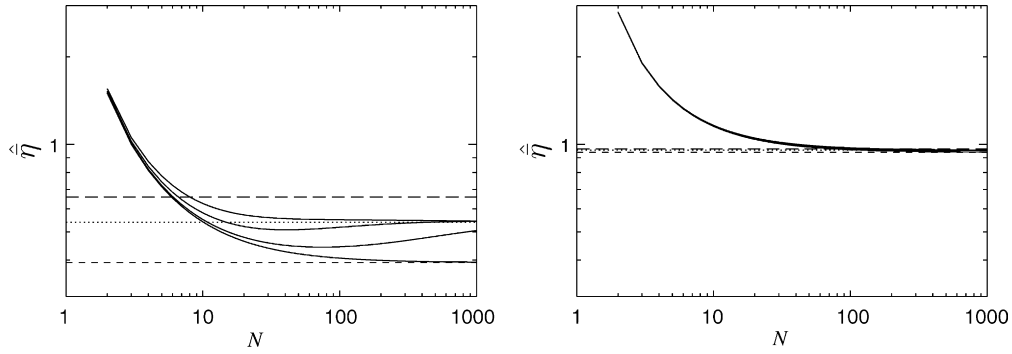


Fig. 5. Calculation of the elongational viscosity as a function of the number of beads for constant Wi and α using the first two terms in the asymptotic expansion for the FENE force law with $\lambda = 1$ (Eq. (30)). The values of Wi are 1 (left) and 10 (right). The lines correspond to different values of α , from top to bottom ranging from 100, 400, 4000, and ∞ . The dashed line is $1 - 6/(\pi^2 Wi)$ (Eq. (31)). The dotted line is $1 - 0.46/Wi$ (Eq. (32)). The long-dashed line is $1 - 0.34/Wi$ (from Eq. (36)).

spring force laws and criteria for the effective persistence length. Since it is an expansion for large strain rates, for sufficiently large strain rates it will eventually describe the response.

Recall that for the FENE force law we have chosen to define A_{true} as one-third of the Kuhn length such that $\nu = \ell/A_{\text{true}}$ is three times the number of Kuhn lengths represented by a spring. While this choice will affect the look of the equation written in terms of ν , the physical meaning is unchanged. We now rearrange and include an approximate form for the longest relaxation time to obtain

$$\hat{\eta} \approx \frac{N+1}{N-1} - \frac{12}{N(N-1)2 \sin^2(\pi/(2N))Wi} \times \frac{1}{4\nu/\lambda + 1.05\sqrt{\nu/\lambda} + 21.1} \left[\frac{\nu}{\lambda} + 4 - \frac{3}{N-1}C_N \right] + \mathcal{O}\left(\frac{1}{Wi^2}\right). \quad (30)$$

We can now analyze how this expansion (the response of the chain) changes as the number of beads is changed while the Weissenberg number Wi is held constant, and $\alpha = (N-1)\nu$ is held constant. When analyzing the behavior we must decide which criterion for choosing λ will be used. We will start by choosing $\lambda = 1$. Note though that this does not correspond to either the high-force or low-force criterion.

Fig. 5 shows plots of Eq. (30) as a function of N for constant Wi and α for $\lambda = 1$, i.e. not using an effective Kuhn length. We see similar shapes as with the previous bead-spring chains discussed. If $1 \ll N \ll \alpha$ we see a plateau which occurs at a viscosity of

$$1 - \frac{6}{\pi^2 Wi} + \mathcal{O}\left(\frac{1}{Wi^2}\right). \quad (31)$$

For all chains with a finite α , the number of beads will eventually become large enough that the springs represents very small segments of polymer. The system then approaches the limiting behavior of the bead-string chain when $1 \ll N$ and $\alpha \ll N$ which is approximately

$$1 - \frac{0.46}{Wi} + \mathcal{O}\left(\frac{1}{Wi^2}\right). \quad (32)$$

This equation is only known approximately because there is some uncertainty in the longest relaxation time of a bead-string chain used to write the expression using a Weissenberg number. Because the difference in responses between the long chain plateau (Eq. (31)) and the bead-string chain (Eq. (32)) decreases with Wi , as Wi^{-1} , the elongational viscosity is less sensitive to the incorrect and changing accuracy of the spring force law as Wi increases.

Recall that for the FENE force law, even the high-force criterion is not $\lambda = 1$. We show in Fig. 6 the response of the elongational viscosity for the high-force and the low-force criteria [7]. The different criteria can only be used up to values of N such that the chain becomes the bead-string chain (i.e. $\lambda \rightarrow \infty$). At this point in N , the curves for the low and high-force criteria must stop. We see that the high-force criterion performs slightly better (stays in the plateau longer) than the low-force criterion, although the difference for the FENE force law is almost indistinguishable. However, there is the counter-intuitive result that using $\lambda = 1$ seems to do even better than either criteria. This can be understood by looking at the expansion in Eq. (30). The coefficient to Wi^{-1} only depends on the ratio ν/λ . Therefore, the smaller the value of λ , the larger the ratio ν/λ , and the closer

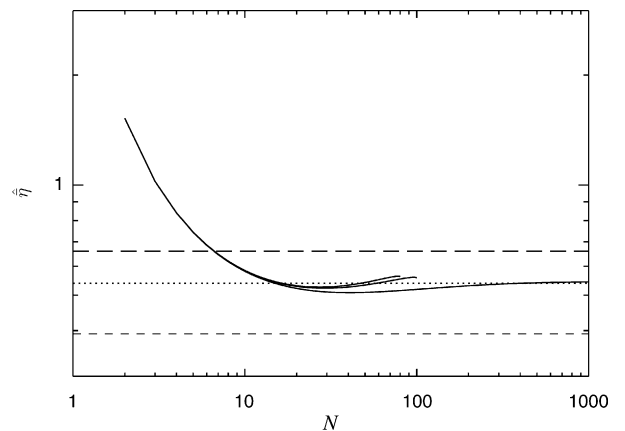


Fig. 6. Comparison of the different criteria for λ and their effect on the elongational viscosity for the FENE force law using Eq. (30). The parameters are $Wi = 1$, $\alpha = 400$, and either the low-force (upper curve) or high-force criteria (middle curve) for λ or $\lambda = 1$ (lower curve). The $\lambda = 1$ case and the dashed, dotted, and long-dashed lines are identical to those in Fig. 5.

the term is to the long chain limit behavior. In essence, a smaller λ makes it look like there are more effective Kuhn lengths per spring, so the chain looks like a chain with a very large number of Kuhn lengths. This arbitrary change of the Kuhn length does not cause a detrimental response in the strong stretching limit because the long chain behavior does not explicitly depend on the true Kuhn length, only on the total drag on the chain, the contour length squared, and the Weissenberg number. Although arbitrarily choosing λ very small does increase the size of the plateau, we do not consider that a viable option for developing an accurate coarse-grained model because the change in effective persistence length would cause all equilibrium properties to be incorrect.

To this point we have presumed that the existence of the plateau in the viscosity means that the chain is an accurate coarse-grained model. For the FENE force law this plateau essentially exists when the chain has many beads but each spring still represents a large segment of polymer. We have shown that even if the incorrect spring force law is used when each spring represents a small segment of polymer, for sufficiently high Wi the elongational viscosity does not actually deviate a significant percentage from the plateau because the chain is always virtually fully extended. However, the existence of this plateau does not in itself guarantee that the bead-spring represents the desired micromechanical model. For the FENE chain, we can easily see how well this plateau matches the behavior of the freely jointed chain because the steady state behavior of the freely jointed chain in elongational flow is known [22]. The expansion of the steady state elongational viscosity of a freely jointed chain for large strain rates is

$$\frac{\bar{\eta} - 3\eta_s}{n_p \zeta a^2} \sim \frac{N(N^2 - 1)}{12} - \frac{k_B T}{\zeta a^2 \dot{\epsilon}} [2(N - 1) - 3C_N] + \mathcal{O}\left(\frac{1}{\dot{\epsilon}^2}\right), \quad (33)$$

where a is the length of a rod and the sum over the Kramers matrix which was tabulated by Hassager can be written equivalently as a simpler sum, C_N . Currently we are concerned with the limit of a large number of rods because we want to compare this series expansion with the plateau occurring for a FENE chain with a large number of springs and where each spring still represents a large number of Kuhn lengths. In the limit of a large number of rods, the elongational viscosity of a freely jointed chain becomes

$$\hat{\eta} \sim 1 - \frac{24}{Wi} \frac{k_B T \tau}{N^2 \zeta a^2} + \mathcal{O}\left(\frac{1}{Wi^2}\right). \quad (34)$$

From ref. [23] we know that the relaxation time of long freely jointed chains is approximately

$$\tau \approx 0.0142 N^2 \frac{\zeta a^2}{k_B T}, \quad (35)$$

so the viscosity is

$$\hat{\eta} \approx 1 - \frac{0.34}{Wi} + \mathcal{O}\left(\frac{1}{Wi^2}\right). \quad (36)$$

We expect that Eq. (31) would be the same as this freely jointed chain result, Eq. (36), however we see that they are not the same. Recall that the FENE force law does not have the exact same behavior as the inverse Langevin function near full extension. This will account for some of the difference, which we will now address by examining the behavior of the Cohen spring force law.

Because the Cohen spring force law does have the same approach to full extension as the inverse Langevin function, but different from the FENE force law, we will be able to see the influence of this divergence. Note that because the first two terms in the flow expansion (in terms of Pe) only depends on the dominant behavior of the spring near full extension, the Cohen force law has the same two term expansion as a bead-spring chain with the inverse Langevin function as the spring force law. Obviously higher order terms in the expansion will be different between the Cohen force law and the inverse Langevin function. The equilibrium behavior (and relaxation time) will also be different at intermediate ν . At infinite ν it only depends on the linear region of the force law which is the same, and at zero ν they both become the bead-string chain which are the same. The first two terms in the high strain rate expansion are

$$\bar{\eta} \sim \bar{\eta}_\infty - \frac{1}{Pe} \left[\left(\frac{2\nu}{3\lambda} + 4 \right) (N - 1) - 3C_N \right] + \mathcal{O}\left(\frac{1}{Pe^2}\right). \quad (37)$$

In the limit of $1 \ll N \ll \alpha$, the expansion becomes

$$\hat{\eta} \sim 1 - \frac{4}{\pi^2 Wi} + \mathcal{O}\left(\frac{1}{Wi^2}\right), \quad (38)$$

where we have used our knowledge of the relaxation time of the bead-spring chain when ν is very large. We can also look in the limit of such large N that each spring represents a very small amount of polymer, $1 \ll N$ and $\alpha \ll N$. In this limit the chain looks like a bead-string chain, which is the same result as for the FENE chain. In this limit the expansion is approximately

$$\hat{\eta} \approx 1 - \frac{0.46}{Wi} + \mathcal{O}\left(\frac{1}{Wi^2}\right). \quad (39)$$

Recall that the approximation here in determining the expansion for the bead-string chain is that the longest relaxation time is only known approximately.

There are two important aspects to notice about the behavior of the Cohen force law chain. The first is that the structure has changed from that of the FENE force law in that Eq. (38) is now greater than Eq. (39). The other is that even this expansion (which is the expansion for the exact inverse Langevin function) deviates from the freely jointed chain result when there are a large number of springs and each spring represents a large segment of polymer (i.e. comparing Eqs. (36) and (38)).

This deviation, however, turns out to be related back to a subtlety with the longest relaxation time of the freely jointed chain which is not often discussed. Consider a freely jointed chain with such a large number of rods that if one models it with a bead-spring chain with the exact inverse Langevin force law, it is possible to both have a very large number of springs and at

the same time have each spring represent a very large number of rods. The longest relaxation time of this bead-spring chain is given by Eq. (12) or alternatively (with $\lambda = 1$)

$$\tau = \frac{(N\zeta)L\alpha_K}{6\pi^2 k_B T}. \quad (40)$$

We know this relaxation time exactly because if each spring represents a very large segment of polymer, near equilibrium the spring only samples the linear region of the force law so we can use the analytic result for the relaxation time of a bead-spring chain with linear springs. Because this bead-spring chain correctly models the equilibrium and force-extension behavior of the freely jointed chain, one might think that it would model the longest relaxation time of the chain. However, this is not true. The longest relaxation time is given in Eq. (35) or equivalently

$$\tau = \frac{0.0142(N\zeta)L\alpha_K}{k_B T}. \quad (41)$$

It is this difference in relaxation times that causes the difference between the viscosity expansion of the freely jointed chain and the Cohen or inverse Langevin chain even when the bead-spring chain has a large number of springs and each spring represents a large segment of polymer. We can see this by using Eq. (40) in the expansion of the freely jointed chain, Eq. (34), instead of the exact formula, which is then identical to the Cohen chain expansion, Eq. (38). We can also see that it is the relaxation time that causes this final discrepancy by noticing that both the freely jointed chain and Cohen chain can be written in these limits as

$$\begin{aligned} \frac{\bar{\eta} - 3\eta_s}{n_p} &\sim \frac{(N\zeta)L^2}{12} - \frac{k_B T}{\dot{\epsilon}} \\ &\times [2 \times (\text{number of Kuhn lengths in whole molecule})] \\ &+ \mathcal{O}\left(\frac{1}{\dot{\epsilon}^2}\right). \end{aligned} \quad (42)$$

It is only when the extension rate is written in terms of a Weissenberg number using different longest relaxation times that gives this final discrepancy.

It should be noted that it is not only from ref. [23] that we know the longest relaxation time of a freely jointed chain. Other researchers [24–26] have performed similar simulations verifying the same result as well as independent tests of the relaxation time. This is also not the first mentioning of this discrepancy [25,26]. The almost 20% deviation in the longest relaxation time is an unresolved issue and is outside the scope of this article. For the purposes of this article we can not do better than reproducing the expansion in Eq. (42), which depends on the behavior near full extension, and to capture the longest relaxation time if each spring represents a large segment of polymer. Thus, this plateau (Eq. (38)) is considered “accurate” for our purposes. However, even the Cohen force law or the inverse Langevin force law will deviate from this as each spring represents a small segment of polymer, and the chain approaches the bead-string chain.

A new spring force law has been developed such that the bead-spring chain accurately represents the force-extension behavior of the freely jointed chain (Eq. (5)) [8]. We can examine how using this new force law affects the elongational viscosity at

large strain rates. The expansion of the viscosity for this force law is

$$\bar{\eta} \sim \bar{\eta}_\infty - \frac{1}{Pe} \left[\frac{2\nu}{3}(N-1) - 3C_N \right] + \mathcal{O}\left(\frac{1}{Pe^2}\right) \quad (43)$$

This expansion should be compared with the expansion for the Cohen force law or inverse Langevin force law (Eq. (37)). We see that because the new force law correctly represents the behavior at large forces, the expansion in viscosity in terms of Pe is modeled correctly (like when using the high-force criterion for an effective persistence length). The term $2\nu(N-1)/3$ is always equal to two times the total number of Kuhn lengths represented by the chain independent of how few Kuhn lengths each spring represents, just as we saw in Eq. (42). However, the equilibrium behavior is also captured correctly with the new force law. This means that the longest relaxation time will also be captured essentially. Because both are captured correctly, the system will not deviate at high discretization from the plateau.

5.2. Models of the worm-like chain

We now analyze of the response of bead-spring chains used to model the worm-like chain. The most commonly used spring force law to model the worm-like chain is the Marko–Siggia interpolation formula. The expansion of the elongational viscosity for large strain rates using the Marko–Siggia force law is

$$\bar{\eta} \sim \bar{\eta}_\infty - \sqrt{\frac{\nu/\lambda}{2Pe}} \sum_{k=1}^{N-1} \sqrt{k(N-k)} + \mathcal{O}\left(\frac{1}{Pe}\right). \quad (44)$$

To investigate the exact chain response and the range of validity of the expansion we performed BD simulations of chains without EV and HI from approximately $Wi = 1$ to 1000 for a range of parameters of the Marko–Siggia force law. These are shown in Fig. 7. We plot the data versus Peclet number instead of Weissenberg number because the Peclet number is the natural parameter in the expansion and simulations. The Peclet number

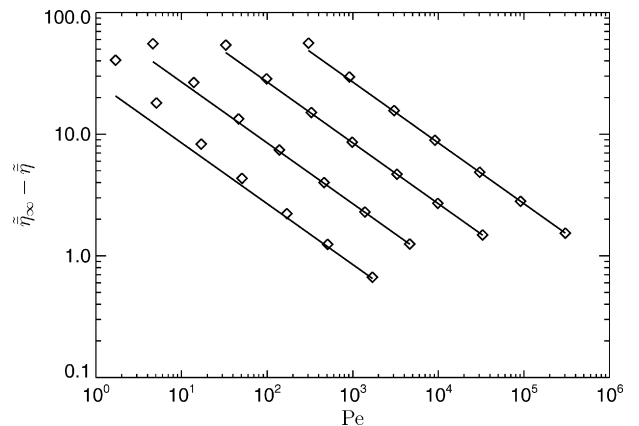


Fig. 7. Comparison of the approach to the plateau elongational viscosity between BD simulations and the two-term series expansion in Eq. (44)(solid lines). The spring force law is the Marko–Siggia formula and the chains consist of 10 beads. The curves correspond to (from left to right) $\nu = 1, 10, 100, 1000$. Each curves spans strain rates from approximately $Wi = 1$ to $Wi = 1000$.

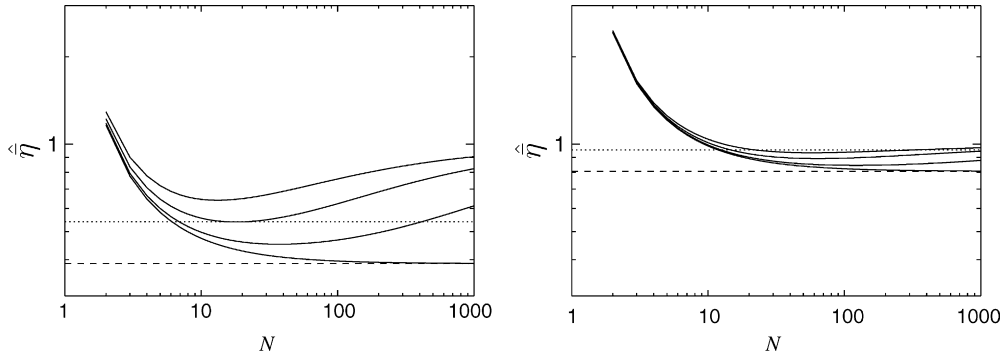


Fig. 8. Calculation of the elongational viscosity as a function of the number of beads for a constant Wi and α using the first two terms in the asymptotic expansion for the Marko–Siggia force law with $\lambda = 1$ (Eq. (48)). The values of Wi are 1 (left) and 10 (right). The lines correspond to different values of α , from top to bottom ranging from 100, 400, 4000, and ∞ . The dashed line is $1 - \sqrt{3/(8Wi)}$ (Eq. (49)), and the dotted line is $1 - 0.46/Wi$ (from Eq. (53)).

is a local comparison of the strain rate to the characteristic time for a bead to diffuse the fully extended length of a spring. In absence of an exact formula for the longest relaxation time in terms of model parameters (an approximate one is given in the previous section) there exists an uncertainty in the value of the Weissenberg number. There is also variability in what characteristic time that is used to define the Weissenberg number. In our comparison of the simulations and expansion we choose to eliminate the uncertainty of the Weissenberg number as a possible source of deviation.

Having verified that the expansion represents the high extension rate behavior of the Brownian dynamics simulations, we can examine the behavior of the two term expansion. We will use the analytic nature of the expansion to investigate the behavior of different bead-spring chains. After the analysis we will return to the question of whether the expansion accurately represents the data over the entire range of analysis. As in ref. [7] we will examine the viscosity as a function of the number of beads while the total number of persistence lengths in the molecule is held constant. We will also keep the Weissenberg number constant as we change the number of beads. We manipulate Eq. (44) to write the expansion as a scaled elongational viscosity in terms of the Weissenberg number

N range so is not a dominant effect. We can replace this by the asymptotic value of $3/2$ without significant error. Similarly, we can replace the relaxation time using the approximation in Eq. (21) which represents the relaxation time to within an error of about a few percent

$$\hat{\eta} \approx \frac{N+1}{N-1} \left(1 - \frac{3}{2} \sqrt{\frac{1}{Wi(6 + 7.26\sqrt{\lambda/v} + 21.2\lambda/v)}} \right) + \mathcal{O}\left(\frac{1}{Wi}\right). \quad (48)$$

With Eq. (48) we have a simple approximation to the response written in terms of Wi . We show in Fig. 8 the value of Eq. (48) as a function of the number of beads, N , for $Wi = 1$ and $Wi = 10$ and using the high-force criterion [7] for the effective persistence length ($\lambda = 1$). The curves are also at a constant total number of persistence lengths, $\alpha = L/A_{\text{true}} = \nu(N-1)$. Although we do not expect Eq. (48) to accurately represent the simulations down to $Wi = 1$ over the whole range of N , the larger spread of the curves allows one to see better the shape of the curves. The behavior at low number of beads is similar to the zero Weissenberg number response, which we again attribute to the fact

$$\hat{\eta} \sim \frac{N+1}{N-1} \left(1 - \frac{6}{N \sin(\pi/(2N))} \frac{\sum_{k=1}^{N-1} \sqrt{k(N-k)}}{N^2-1} \sqrt{\frac{\hat{\tau} 2 \sin^2(\pi/(2N)) \nu/\lambda}{Wi}} \right) + \mathcal{O}\left(\frac{1}{Wi}\right), \quad (45)$$

where we have defined a dimensionless relaxation time as

$$\hat{\tau} = \tau \left(\frac{k_B T}{\xi \ell^2} \right). \quad (46)$$

The prefactor

$$\frac{6}{N \sin(\pi/(2N))} \frac{\sum_{k=1}^{N-1} \sqrt{k(N-k)}}{N^2-1} \quad (47)$$

ranges from $\sqrt{2}$ for both $N = 2$ and $N = 3$ to $3/2$ for $N \rightarrow \infty$. This prefactor changes by a total of about 6% over the entire

that the hydrodynamic drag is exerted only on discrete beads instead of along a continuous contour. If the chain is very long ($\alpha \gg 1$), there will exist a large region for which $1 \ll N \ll \alpha$ and the viscosity is

$$1 - \sqrt{\frac{3}{8Wi}} + \mathcal{O}\left(\frac{1}{Wi}\right). \quad (49)$$

However, for chains with a finite length (so finite α), N will eventually become large enough that each spring represents a small segment of polymer. The limit of this progression is when $\alpha \ll N$. In the limit that $1 \ll N$ and $\alpha \ll N$, the viscosity

approaches

$$1 + \mathcal{O}\left(\frac{1}{Wi}\right). \quad (50)$$

The difference between Eqs. (49) and (50) decreases as $Wi^{-1/2}$, which means that for very large Weissenberg number, there is no upper limit on the number of beads past which the response deviates significantly. Essentially, if the Weissenberg number is large enough, the chain will be almost fully extended and so even if the spring force is not represented correctly, the chain will still be in the fully extended state. Thus, for some properties the change if the incorrect spring force law is used may appear to have a negligible effect. Note that this is different from the low Weissenberg number behavior which was found to have a maximum number of beads of $N^{1/2} \ll 1.15\alpha^{1/2}$ for the Marko–Siggia spring force law [7]. This means that the response of the bead-spring chain seems to be less sensitive to using an inappropriate spring force law when the springs become very small.

To this point we have not used an effective persistence length that differed from the persistence length of the WLC being modeled, thus $\lambda = 1$. Recall the progression of analysis used to study the behavior at low Wi [7]. The analysis with $\lambda = 1$ showed that there was an error in the low Wi response if each spring represented too small an amount of polymer. However, if the low-force criterion was used for the effective persistence length, the error due to the incorrect force law vanished in the range of applicability of the low-force criterion. The only error that remained was from the fact that for small number of beads, the drag was not distributed along the contour. We would thus expect that a similar vanishing of the error would be present in this case if the high-force criterion were used. But recall that for the Marko–Siggia force law using $\lambda = 1$ is the high-force criterion. There is still a deviation when each spring represents too few number of persistence lengths. Let us compare this response if instead λ were chosen according to the low-force criterion. This response is shown in Fig. 9. Recall that as the number of beads N is increased, the number of persistence lengths per spring,

ν , decreases. For the low-force criterion, the effective persistence will increase until the point of $\nu = 10/3$ when $\lambda \rightarrow \infty$. At this point, the chain becomes a bead-string chain, and the curve in Fig. 9 can not continue past that value of N . We see that the response with the low-force criterion more quickly deviates from the plateau. Although it is true that the high-force criterion produces a more extended plateau region, there is still an error if each spring represents a small number of persistence lengths.

If we look closer at the expansion we see that the prefactor to $Pe^{-1/2}$, that is $\lambda^{-1/2}$, is correct if the high-force criterion is used and deviates if the low-force criterion is used. However, the plots have been produced at constant Wi . To convert the formula from Pe to Wi the longest relaxation time must be used. This longest relaxation time depends on the low-force behavior of the chain. Recall that the modified Rouse relaxation time is a function of the second moment of the spring length, $\langle r^2 \rangle$, and the low-force criterion gets this second moment correct. Thus, when using the high-force criterion it is the longest relaxation time that deviates at high discretization causing the error, while using the low-force criterion gets the longest relaxation time correct (to within the error between the true relaxation time and the modified Rouse relaxation time) but has an error in the explicit prefactor to the Pe . In some sense this makes the response at high Wi more complicated and a more stringent test of the accuracy of the spring force law because the response has a contribution having to do with the high-force response and one having to do with the low-force response. However, recall that it is also a less stringent test because if the Wi is large enough the chain is fully extended irrespective of the details of the spring force law.

To this point we have used the first two terms in the asymptotic expansion to examine analytically the behavior of the bead-spring chains. We have gained significant knowledge about the response of the bead-spring chains using an expansion that is relatively simple to produce and will be valid at large enough strain rates. We now return to a more detailed description of how accurately the two terms represents the true response of the bead-spring chains. To answer that question, we will examine the higher order terms in the expansion. The Pe^{-1} correction to Eq. (44) can be calculated with some effort, but the $Pe^{-3/2}$ term is excessively complex. However, we can use knowledge of the structure of the series and our BD simulations to generate an *approximate* form for the $Pe^{-3/2}$ term. These two corrections to Eq. (44) are

$$\begin{aligned} & \frac{-1}{Pe} \left[\frac{7}{2}(N-1) - 3C_N \right] \\ & - \frac{1}{Pe^{3/2}} \left[3.6\sqrt{\frac{\lambda}{\nu}} + \sqrt{\frac{\nu}{\lambda}} + \left(1 - \frac{2}{N^2}\right) \left(\frac{\nu}{\lambda}\right)^{3/2} \right]. \quad (51) \end{aligned}$$

While the $Pe^{-3/2}$ term is only approximate, with the addition of these two terms, the expansion models well the response of chains with $N = 2, 5, 10, 30$ and $\nu/\lambda = 1, 10, 100, 1000$ for flows ranging from $Wi = 1$ to $Wi = 1000$. The expansion has a typical error of 2% for $Wi = 1$ with a much smaller error for higher Wi . Using this, we can find the next corrections to Eqs. (49) and (50). The next correction for Eq. (49) comes from exam-

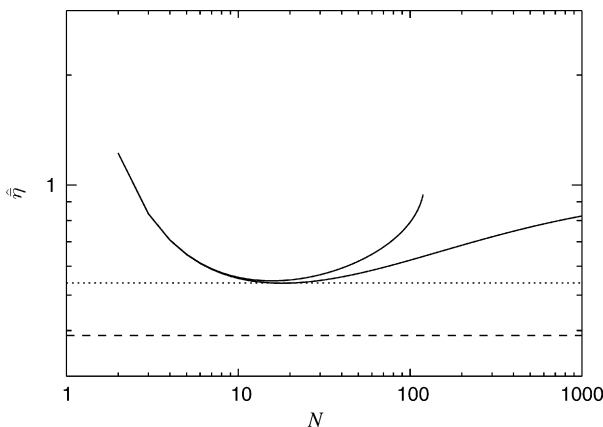


Fig. 9. Comparison of the different criteria for λ and their effect on the elongational viscosity for the Marko–Siggia force law using Eq. (48). The parameters are $Wi = 1$, $\alpha = 400$, and either the low-force (upper curve) or the high-force criteria (lower curve) for λ . The high-force criterion curve and the dashed and dotted lines are identical to those in Fig. 8.

ining the limit $1 \ll N \ll \alpha$. In that limit the Wi^{-1} term vanishes and the $Wi^{-3/2}$ term becomes

$$\frac{-0.07}{Wi^{3/2}}, \quad (52)$$

where the possible error in the coefficient results because this term was only inferred from the simulations. While this correction will play a role if the Wi is not large enough, it should play a secondary role and the qualitative behavior discussed previously will remain unchanged. The correction for Eq. (50) is more subtle. When only using the first two terms in the expansion, the $Wi^{-1/2}$ term vanishes in the limits $1 \ll N$ and $\alpha \ll N$ as the chain approaches the bead-string chain. Therefore, we only capture the finite extensibility but not the approach to finite extensibility. In this limit the $\mathcal{O}(1)$ term is modeled correctly, but the $\mathcal{O}(Wi^{-1/2})$ term of the worm-like chain is not. To examine this limit we must examine the higher terms in the expansion. However, we see that the coefficient to the $Wi^{-3/2}$ term actually diverges. This happens because the limit to a bead-string chain is a singular limit. It is similar to the force-extension behavior at large force using the Marko–Siggia spring force law. Thus, the Pe^{-1} term in Eq. (51) is the behavior seen if, for a constant ν/λ , the Pe is made large. If instead the limit $\nu/\lambda \rightarrow 0$ is taken for a constant Pe or Wi , the response should approach the bead-string chain. If this bead-string chain response is expanded for large Pe or Wi , the Pe^{-1} term is different than in Eq. (51). The coefficient to Pe^{-1} depends on the order in which the limits are taken. We have already seen the expansion of the bead-string chain (if $\nu/\lambda \rightarrow 0$ in Eq. (25)) which has a Pe^{-1} term that is similar to the one in Eq. (51) but with the $7/2$ replaced by a 4. Thus, in the limit $1 \ll N$ but $\alpha \ll N$ the true next correction to the response of the Marko–Siggia bead-spring chains as seen in Figs. 8 and 9 is

$$\frac{-0.46}{Wi}, \quad (53)$$

where the possible error in this coefficient results from using our approximate formula for the relaxation time (used to convert from Pe to Wi) in the limit $\nu/\lambda \rightarrow 0$.

We have now examined the next corrections to the behavior in the two different limits, both $1 \ll N \ll \alpha$ and $1 \ll N$ and $\alpha \ll N$. While these obviously affect the quantitative comparison between the curves in Figs. 8 and 9, the qualitative nature will not be changed significantly because at a large enough Wi only the first two terms in the expansion are sufficient to describe the simulation results.

The analysis of the Marko–Siggia force law has shown that the response does begin to deviate at large enough discretization because each spring represents too small a segment of polymer. In this limit the Marko–Siggia spring force law does not accurately capture the response of the worm-like chain it is trying to represent. A new spring force law has been developed which can be used to model a worm-like chain even if each spring represents as few as 4 persistence lengths (provided the whole chain contains many persistence lengths) [9]. This new force law was given in Eq. (2). The expansion of the elongational viscosity

using this new spring force law for the worm-like chain is

$$\tilde{\eta} \sim \tilde{\eta}_\infty - \sqrt{\frac{\nu}{2Pe}} \sum_{k=1}^{N-1} \sqrt{k(N-k)} + \frac{3C_N}{Pe} + \mathcal{O}\left(\frac{1}{Pe^{3/2}}\right). \quad (54)$$

We can explicitly see from this expansion the great advantage of the new spring force law. Note that the $Pe^{-1/2}$ term looks like that for the Marko–Siggia force law using the high-force criterion for the effective length, while the new force law does not need to use an effective persistence length. Previously we saw that even using the high-force criterion and the Marko–Siggia force law, the response deviated at high discretization because the longest relaxation time (used to convert from Pe to Wi) did not correctly compensate for the ν in the expansion. Using the idea of a modified Rouse relaxation time, we can understand that essentially the relaxation time deviated because the size of the spring at equilibrium ($\langle r^2 \rangle$) was incorrect. However, the new spring has by construction the correct equilibrium ($\langle r^2 \rangle$). To within the accuracy of the modified Rouse relaxation time, the longest relaxation time will be correctly modeled even at high discretization.

The other advantage of the new spring force law is the order Pe^{-1} term. In developing the new force law, the coefficient to the $\hat{r}/(1-\hat{r}^2)$ term in the force law was determined such that the f^{-1} term in the force-extension behavior near large force would vanish (which it does for very long worm-like chains). While this choice does not make the Pe^{-1} term vanish here in the elongational viscosity, the coefficient is made $\mathcal{O}(1)$ instead of $\mathcal{O}(N)$ which is a significant reduction when N is large. Recall that N must be large to even be in the plateau region of discretization. We postulate that the true continuous worm-like chain would not have a Pe^{-1} term just as it did not have a f^{-1} term in the force-extension behavior. Thus, even at the next order in the expansion having the correct force-extension behavior corresponds to having the correct behavior in elongational flow.

Finally, we can compare between the response of freely jointed chains and worm-like chains. Consider a worm-like chain with $\alpha = 400$ persistence lengths at a $Wi = 10$. Fig. 10 shows the elongational viscosity using the Marko–Siggia force law with $\lambda = 1$ as a function of the number of beads used in the model. The curve plotted is from Eq. (48) with the additional terms from Eq. (51). We also show in Fig. 10 the response of chains using the FENE spring force law attempting to model the worm-like chain. It is important to note that FENE chain used to model a worm-like chain with 400 persistence lengths would have $\alpha = 600$ (i.e. there are 200 Kuhn lengths, so three times the number of Kuhn lengths is 600). In Fig. 10 we plot Eq. (30) for the FENE force law with $\alpha = 600$, $Wi = 10$, and $\lambda = 1$.

This figure illustrates the difference in response between the two force laws and the different micromechanical models at large Wi . The weaker approach towards maximum elongational viscosity as $Wi^{-1/2}$ for the worm-like chain results in a smaller elongational viscosity than the freely jointed chain, which approaches as Wi^{-1} . However, as each model is more finely discretized, both eventually approach the same model, the bead-string chain.

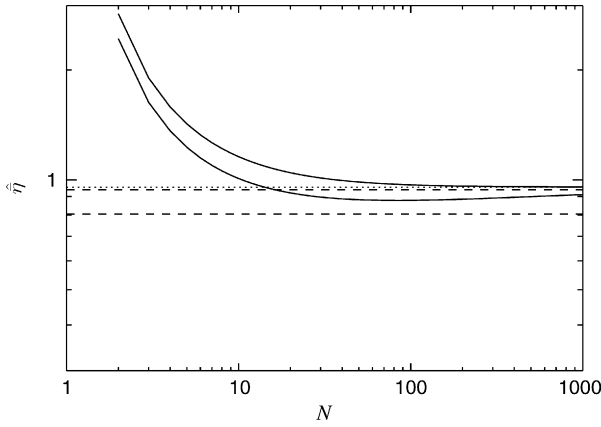


Fig. 10. Comparison of the elongational viscosity between models using the Marko–Siggia vs. FENE force laws. The solid lines correspond to Marko–Siggia (lower, Eq. (48) modified with Eq. (51)) and FENE (upper, Eq. (30)). The models contain 400 persistence lengths ($\alpha = 400$ for Marko–Siggia, $\alpha = 600$ for FENE) and are at $Wi = 10$ with $\lambda = 1$. The dotted line represents the bead-string result (Eq. (32)). The dashed lines represent the plateau regions for Marko–Siggia (lower, Eq. (49)) and FENE (upper, Eq. (31)).

In this section we have analyzed the behavior of bead-spring chains in uniaxial elongational flow at large strain rates. After verifying the applicability of the expansion for large strain rates, we could use the expansion to better understand the physical origin of the chain response. We found that if the strain rate is large enough, the chain is essentially fully extended and so the elongational viscosity is the fully extended value virtually independent of the accuracy of the spring force law. However, the “deficit”, or how close the system is to that plateau, does depend on the accuracy of the spring force law. In fact the accuracy of this deficit is even more subtle to understand than the weak flow response. The response certainly depends on the behavior of the spring near full extension which is shown by the expansion of the viscosity in terms of Pe . However, it is conventional to express the expansion in terms of a Weissenberg number, which uses the longest relaxation time. This longest relaxation time depends on the equilibrium response of the spring, not the response near full extension. To get the correct behavior for the deficit a model should get both behaviors correct, at large forces and at equilibrium. For the Marko–Siggia spring force law, neither the low-force nor the high-force criteria capture correctly the response at both extremes. For this reason the deficit is incorrect if very small springs are used. However, our new spring force law does get the behavior correct at low force and high force, and thus represents the deficit correctly even to high discretization provided the number of beads is large enough.

It is useful to review at this point the main features we have observed through the analysis of the elongational viscosity at large strain rates. At very large strain rates the chain is virtually fully extended, so as long as the spring has the correct fully extended length ℓ , this infinite strain rate viscosity is independent of the details of the spring force law. In this sense the behavior at large enough strain rate is insensitive to the details of the spring force law. However, some experiments may aim to explore more than the absolute value of viscosity (or similarly fractional extension). For example, ref. [27] used the deficit (dif-

ference between the fractional extension from full extension) to distinguish between the worm-like chain, freely jointed chain, and stem-flower models. Shaqfeh et al. [28] and Doyle et al. [29] examined the relaxation after strong elongational flow and found that the relaxation was highly influenced by the deficit away from the fully extended state. For a bead-spring chain to accurately represent these types of response of a micromechanical model, it is necessary to capture not only the plateau but also the approach to the plateau. This approach is sensitive to the accuracy of the spring force law. In fact it is dependent on the force law both near full extension and at equilibrium because of using the longest relaxation time to form a Weissenberg number. For this reason previously used spring force laws do not capture this deficit when each spring represents a small segment of polymer. However, the new spring force laws developed to represent the worm-like chain and freely jointed chain do not deviate at high discretization.

6. Influence of hydrodynamic interactions

In this article we have focused on the role of the spring force law and have not included effects of hydrodynamic interactions. In highly extended states we expect the effect will be much less than in the coiled state, and the spring force law will play the major role. For the Marko–Siggia force law, we found that the elongational viscosity has a series expansion of the form

$$\frac{\bar{\eta} - 3\eta_s}{n_p \zeta \ell^2} \sim \frac{N(N^2 - 1)}{12} \left(1 - \frac{C}{Pe^{1/2}} + \mathcal{O}\left(\frac{1}{Pe}\right) \right). \quad (55)$$

Certainly the plateau value will be dependent on hydrodynamic interactions, which changes the scaling with length to include a logarithm. However, we postulate the coefficient C may have the same scaling with or without hydrodynamic interactions. This is because the chain is so close to full extension that the positions of the beads, and therefore their interactions, will not be much different from in the fully extended state. The postulated form is thus

$$\bar{\eta} - 3\eta_s \sim (\bar{\eta} - 3\eta_s)_\infty \left(1 - \frac{C}{Pe^{1/2}} + \mathcal{O}\left(\frac{1}{Pe}\right) \right). \quad (56)$$

Whether the scaling of C is the same with and without hydrodynamic interactions has interesting consequences. Without hydrodynamic interactions the scaling is $C \sim N^{-1}$. This is consistent with turning the Peclet number into a Weissenberg number, because without HI the longest relaxation time scales as N^2 . However, in the non-draining limit, the longest relaxation time scales as $N^{3/2}$. Turning the expansion Pe to Wi using a non-draining scaling for the longest relaxation time gives a coefficient of

$$\frac{CN^{3/4}}{Wi^{1/2}}. \quad (57)$$

If the value of C scales as N^{-1} , this implies a vanishing coefficient to $Wi^{-1/2}$ as $N \rightarrow \infty$.

To test this hypothesis, we performed simulations using the Marko–Siggia force law and the RPY hydrodynamic interaction tensor, with parameters $\nu = 200$, $\lambda = 1$, and $h^* = 0.25$ [2]. We

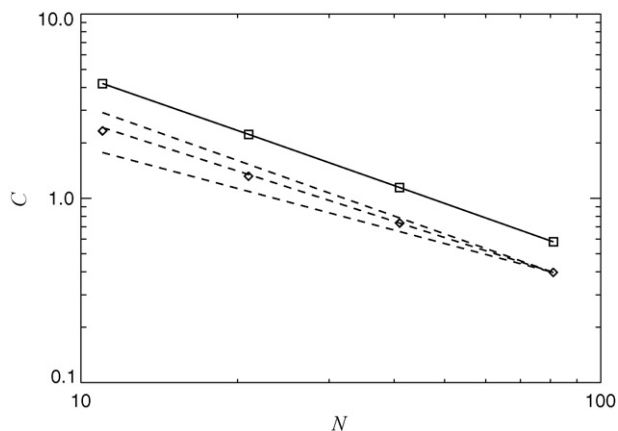


Fig. 11. Coefficient of the $Pe^{-1/2}$ term, C , as a function of the number of beads with and without HI. The spring force law is Marko–Siggia with $\nu = 200$ and $\lambda = 1$. The squares are without HI and the diamonds are from BD simulations using the RPY tensor and $h^* = 0.25$. The dashed lines represent power laws of N^{-1} , $N^{-0.9}$, and $N^{-0.75}$.

performed simulations at a range of Pe until we were confident that higher order terms in Pe were negligible and extracted a value of C from the simulation data. The infinite Pe number response was calculated exactly using the formalism presented in an appendix to ref. [3]. In Fig. we plot the value of C calculated from the simulations versus N . From the figure we can see clearly that the scaling is not $N^{-3/4}$. The fitted scaling is approximately $N^{-0.90}$ for the largest N simulated here.

These simulations bring about an interesting point which warrants further investigation. If the scaling of C with N in the large chain limit is different than $N^{-3/4}$ as we see here, that means that near the fully extended state the time used to convert from Pe in order to have collapse of the data in the long chain limit is not the longest relaxation time. However, it may be necessary to reach the non-draining limit in the extended state in order to reach the long chain limit scaling of the coefficient. By non-draining limit in the extended state, we mean that the plateau viscosity scales as would be expected from Batchelor's formula. We can estimate the number of beads necessary to be in that limit using an approximate formula in the appendix of ref. [3]. Because of the slow logarithm convergence in the number of beads, with the parameters used here, the number of beads would have to be greater than 10^6 to be into the non-draining limit in the extended state. This is not feasible to simulate. A better route to reach the non-draining limit would be make each spring represent a smaller segment of polymer. However, care should be taken to make sure the correct h^* is used relative to the size of a spring.

7. Conclusion

In this article we have looked at the behavior of bead-spring chain models in strong flows and the effect of the spring force law. We did this for coarse-grained models of both the WLC and FJC. We expect that EV effects are small in such strong flows and the effects of HI may be small (or smaller) so we initially neglect those contributions. The longest relaxation time was examined, which is used to express the strain rate as a Weissenberg number.

It was shown that the chain samples the nonlinear regions of the force law even at equilibrium, making the relaxation time deviate from the Rouse result. However, a modified Rouse model is able to capture the relaxation time even if each spring represents a small segment of polymer. This modified Rouse model gives insight into the important role the force-extension behavior at small force plays in determining the longest relaxation time.

We looked at the elongational viscosity in the limit of large strain rates and used the first few terms in the expansion to understand how the response of the chain changes as the level of discretization changes and for different spring force laws. We basically saw that for arbitrarily large strain rate the viscosity becomes not as sensitive to getting the spring force law correct because the system is always fully extended. However, it is important to model correctly how close the chain is to fully extended. To get this correct it is even more sensitive than in weak flows/equilibrium. This is because you are in a highly extended state so the expansion depends on that behavior, but also when writing the response in terms of a Wi with the longest relaxation time, that is influenced by the low-force/equilibrium behavior. So to really get the correct response you need to get both correct. Using the previous force laws with an effective persistence length requires a trade-off to get one right or the other but not both. Our new force laws get both correct so do not deviate when each spring represents a small segment of polymer.

Acknowledgements

This work was supported by the National Science Foundation CAREER program Grant No. CTS-0239012 and P.S.D's Doherty Chair. We also acknowledge Chih-Chen Hsieh for help performing the simulations including hydrodynamic interactions.

References

- [1] R.M. Jendrejack, J.J. dePablo, M.D. Graham, Stochastic simulations of DNA in flow: Dynamics and the effects of hydrodynamic interactions, *J. Chem. Phys.* 116 (2002) 7752–7759.
- [2] C.-C. Hsieh, L. Li, R.G. Larson, Modeling hydrodynamic interaction in Brownian dynamics: simulations of extensional flows of dilute solutions of DNA and polystyrene, *J. Non-Newtonian Fluid Mech.* 113 (2003) 147–191.
- [3] R. Prabhakar, J.R. Prakash, T. Sridhar, A successive fine-graining scheme for predicting the rheological properties of dilute polymer solutions, *J. Rheol.* 48 (2004) 1251–1278.
- [4] G.C. Randall, K.M. Schultz, P.S. Doyle, Methods to electrostatically stretch DNA: microcontractions, gels, and hybrid gel-microcontraction devices, *Lab Chip* 6 (2006) 516–525.
- [5] J.W. Larson, G.R. Yantz, Q. Zhong, R. Charnas, C.M. D'Antoni, M.V. Gallo, K.A. Gillis, L.A. Neely, K.M. Phillips, G.G. Wong, S.R. Gullans, R. Gilmanshin, Single DNA molecule stretching in sudden mixed shear and elongational microflows, *Lab Chip* 6 (2006) 1187–1199.
- [6] A.G. Balducci, P.S. Doyle, Double-stranded DNA diffusion in slit-like nanochannels, *Macromolecules* 39 (2006) 6273–6281.
- [7] P.T. Underhill, P.S. Doyle, On the coarse-graining of polymers into bead-spring chains, *J. Non-Newtonian Fluid Mech.* 122 (2004) 3–31.
- [8] P.T. Underhill, P.S. Doyle, Development of bead-spring polymer models using the constant extension ensemble, *J. Rheol.* 49 (2005) 963–987.

- [9] P.T. Underhill, P.S. Doyle, Alternative spring force law for bead-spring chain models of the worm-like chain, *J. Rheol.* 50 (2006) 513–529.
- [10] M. Somasi, B. Khomami, N.J. Woo, J.S. Hur, E.S.G. Shaqfeh, Brownian dynamics simulations of bead-rod and bead-spring chains: numerical algorithms and coarse-graining issues, *J. Non-Newtonian Fluid Mech.* 108 (2002) 227–255.
- [11] R.G. Larson, The rheology of dilute solutions of flexible polymers: Progress and problems, *J. Rheol.* 49 (2005) 1–70.
- [12] E.S.G. Shaqfeh, The dynamics of single-molecule DNA in flow, *J. Non-Newtonian Fluid Mech.* 130 (2005) 1–28.
- [13] P. Sunthar, D.A. Nguyen, R. Dubbelboer, J.R. Prakash, T. Sridhar, Measurement and prediction of the elongational stress growth in a dilute solution of DNA molecules, *Macromolecules* 38 (2005) 10200–10209.
- [14] J.F. Marko, E.D. Siggia, Stretching DNA, *Macromolecules* 28 (1995) 8759–8770.
- [15] H.R. Warner, Kinetic theory and rheology of dilute suspensions of finitely extendible dumbbells, *Ind. Eng. Chem. Fundam.* 11 (1972) 379–387.
- [16] A. Cohen, A Padé approximant to the inverse Langevin function, *Rheol. Acta* 30 (1991) 270–272.
- [17] H.C. Öttinger, *Stochastic Processes in Polymeric Fluids: Tools and Examples for Developing Simulation Algorithms*, Springer, Berlin, 1996.
- [18] J. Rotne, S. Prager, Variational treatment of hydrodynamic interaction in polymers, *J. Chem. Phys.* 50 (1969) 4831–4837.
- [19] H. Yamakawa, Transport properties of polymer chains in dilute solution: Hydrodynamic interaction, *J. Chem. Phys.* 53 (1970) 436–443.
- [20] R.B. Bird, R.C. Armstrong, O. Hassager, *Dynamics of Polymeric Liquids volume 1: Fluid Mechanics*, second ed., Wiley, New York, 1987.
- [21] R.B. Bird, C.F. Curtiss, R.C. Armstrong, O. Hassager, *Dynamics of Polymeric Liquids, volume 2: Kinetic Theory*, second ed., Wiley, New York, 1987.
- [22] O. Hassager, Kinetic theory and rheology of bead-rod models for macromolecular solutions I. equilibrium and steady flow properties, *J. Chem. Phys.* 60 (1974) 2111–2124.
- [23] P.S. Doyle, E.S.G. Shaqfeh, A.P. Gast, Dynamic simulation of freely draining flexible polymers in steady linear flows, *J. Fluid Mech.* 334 (1997) 251–291.
- [24] P.S. Grassia, E.J. Hinch, Computer simulations of polymer chain relaxation via Brownian motion, *J. Fluid Mech.* 308 (1996) 255–288.
- [25] F. Peters, *Polymers in flow, modeling and simulation*, Ph.D. Thesis, Delft University of Technology, 2000.
- [26] P. Dimitrakopoulos, Stress and configuration relaxation of an initially straight flexible polymer, *J. Fluid Mech.* 513 (2004) 265–286.
- [27] B. Ladoux, P.S. Doyle, Stretching tethered DNA chains in shear flow, *Europhys. Lett.* 52 (2000) 511–517.
- [28] E.S.G. Shaqfeh, G.H. McKinley, N. Woo, D.A. Nguyen, T. Sridhar, On the polymer entropic force singularity and its relation to extensional stress relaxation and filament recoil, *J. Rheol.* 48 (2004) 209–221.
- [29] P.S. Doyle, E.S.G. Shaqfeh, G.H. McKinley, S.H. Spiegelberg, Relaxation of dilute polymer solutions following extensional flow, *J. Non-Newtonian Fluid Mech.* 76 (1998) 79–110.